International Journal of
INTELLIGENT SYSTEMS AND APPLICATIONS IN ENGINEERING

IJISAE

ISSN:2147-6799 www.ijisae.org Original Research Paper

Detection and Difference of Pneumonia from other Chest/Lung Disease using Multi-model Data: A Hybrid Classification Model

[1]Sravani Nalluri, [2]R. Sasikala*

Submitted: 26/06/2023 **Revised**: 07/08/2023 **Accepted**: 27/08/2023

Abstract: The morbidity and mortality due to pneumonia is drastically increased in the developing countries due to multiple factors like poverty, poor health care, overcrowding, poor hygiene, malnutrition, and air pollution. It is more important to implement the effective diagnostic model, which can assist in detecting & differentiating pneumonia from other lung diseases. Usually, lung disease symptoms do not show up until the disease become severe. Hence, we propose a model that detects pneumonia early with the help of x rays and text data (symptoms and signs). Dataset & proposed model/methods: This work puts up an effort to model a new lung disease classification with multi-modal data, where the information of symptoms is in text form along with X-ray images. Initially, the dataset is collected manually with eight chest diseases in text and image format. And, the size of the dataset is 2286 x 3600 images. And, the steps like pre-processing, feature extraction takes place separately for both text input and image input. Further, improved feature level fusion is performed that combines both the features to determine the final classification. Particularly, statistical features, IG, and improved entropy features will be extracted from the text input. GLCM, MBP, and improved CSLBP features are extracted from the input image. Further, the fused features are subjected to the hybrid classification model that integrates the Deep Maxout and CNN to categorize the lung diseases. Optimal training is carried out in the hybrid classification model via a new CBRACDC (Customized Battle Royale Algorithm with Canberra Distance Calculation) algorithm. Finally, the superiority of the proposed work is evaluated over the conventional models. Results: The proposed model attains an enhanced accuracy as 85.13%, 87.99%, 92.28% and 95.28 % for various learning percentages like 60, 70, 80 and 90 respectively than conventional models. It also achieves better sensitivity, specificity, f value as well as low FPR, FNR and error rate when compared to conventional models. The best result achieved at learning percentage 90. Conclusion: It is concluded that the recommended model has an effective performance than the existing models.

Keywords: *Lung disease detection, Deep Maxout, CNN, CBRACDC; Optimization*

Nomenclature

Abbreviation	Description
COPD	Chronic Obstructive Pulmonary Disease
NN	Neural Network
WHO	World health Organization
RP	Radiation-Induced Pneumonitis
AI	Artificial Intelligence
ML	Machine Learning
CNN	Convolutional Neural Networks
ACDC@LungHP	Automatic Cancer Detection and Classification in Whole-slide Lung Histopathology
CAD	Computer-Aided Diagnosis
WSI	Whole Slide Imaging
Inf-Net	Infection Segmentation Deep Network
CT	Computerized Tomography
DL	Deep Learning
AHHMM	Adaptive Hierarchical Heuristic Mathematical Model
NSCLC	Non-Small Cell Lung Cancers
MRFO	Manta Ray Foraging Optimization
EO	Equilibrium Optimizer
R-CNN	Region based CNN
MBP	Median Binary pattern
CSLBP	Center Symmetric Local Binary Pattern
BRO	Battle Royale Optimization
SD	Standard Deviation
STN	spatial transformer network
CNN	Convolutional neural network
IG	Information Gain
GLCM	Gray-Level Co-occurrence Matrix
LBP	Local Binary Pattern
MBP	Median Binary Patterns
FC	Fully Connected

CapsNet	Capsule Networks
NN	Neural network
DL	Deep learning
WCL	Weighted Categorical Loss
SMOTE	Synthetic Minority Oversampling Technique

1. Introduction

Several forms of investigation have been started worldwide regarding the accuracy of detecting the lung diseases likeCovid-19 infection, pneumonia etc [1] [2]. This is because, for medical professionals, it is difficult to distinguish pneumonia and other lung diseases [3]. Moreover, the investigation becomes very crucial as the impact of disease on humans is rising quickly due to poor air quality, overcrowding, malnutrition, poverty, climate change, and other reasons. In 2016, 3.4 million individuals worldwide passed away from COPD, which is typically caused on by tobacco smoke and pollution, whereas asthma took the lives of 400,000 people. A risk of lung disorders[4] [5] is very high, particularly in low- and middle-income, and developing nations. As a result, action must be taken to lower carbon emissions and air pollution. Also, lung disease detection early is therefore more crucial than ever. ML and DL can be extremely useful in achieving this goal. Digital technology has recently gained importance on a global scale.

Several researchers have done the investigations to diagnose lung diseases from X-ray images due to machine learning and deep learning models [6] [7]. However, [7] [4] computerized diagnostic models often become complicated while dealing with the huge volume of data available publicly, which can be resolved by enhancing the efficiency of the models. On the other hand, [9] researchers put on their efforts on early diagnosis of disease with the help of symptoms and X-ray images. This could enable the system to be even more effective as the model can identify the diseases priorly before it reaches the severity level. [10] [11] [12] Also, this development could help in decreasing the medical costs with the help of computer science technology in the fields of health and medical science projects. This paper takes an effort for the early diagnosis of pneumonia and differentiates with other diseases with multi-modal information, particularly text and X-ray images. Here, texts are the symptoms and signs relating to the diseases. Major contributions of the proposed model are:

- To contribute in the improvement of text features and image features that even makes the system stronger by evaluating appropriate feature set.
- To determine the improved feature level fusion for finalizing the diagnosis results.
- To define the optimal trained hybrid classification model that integrates the concept of deep maxout and CNN model, respectively.
- For effective optimization, a new CBRACDC is introduced in this paper.

The subsequent paper organization is as: Section II shows the Literature survey. Proposed method layout was explained clearly in Section III. Section IV deals with preprocessing, feature extraction, and improved feature level fusion. Section V offers hybrid classification (Averaging Deep Maxout and CNN). Section VI offers recommended CBRACDC algorithm. Section VII explains results and conclusion.

2. Literature Survey

A. Literature review

In 2021, Lam Pham *et al.* [13] explored a useful DL framework for auscultator analysis. This seeks to classify anomalies in respiratory cycles and diagnose illnesses using audio of respiratory sounds. The architecture transforms the receiving noise into a spectrogram form during the front-end phase of feature extraction. Using a back-end DL network, the spectrogram properties were then categorized into groups based on respiratory abnormality cycles or diseases.

In 2022, Faizan Karim*et al.* [14] investigated the use of CapsNets and their incorporation into the classification of chest X-rays. The goal is to use CapsNet to create a deep model that improves the accuracy of the classification problem. To address CNN's drawbacks, a new automated learning architecture called CapsNets has been developed.

In 2020, Muhammad Umer*et al.* [15] provided a method for making predictions using CNN that extracts information from chest x-ray images. Three filters are used to extract the edges from the images, which aid in obtaining the segmented target with the contaminated area of the X-ray that is sought. The Image Data Generator class of Keras is used to create 10,000 enhanced images in order to accommodate the decreased amount of the training dataset.

In 2020, Qiao Ke*et al.* [16] offered an approach to help doctors make decisions faster and more accurately by offering them with decision support. To detect degraded

[1] Research Scholar, Scope School, VIT University, Vellore 632014, India Email: sravani22me@gmail.com
[2] Associate Professor, Scope School, VIT University, Vellore 632014, India E-mail: sasikala.ra@vit.ac.in
** Corresponding Author E-mail: sasikala.ra@vit.ac.in*

Table I- Analysis of Standard Lung Disease Classification from Multi-Model Data			
Author[citation]	**Methods**	**Features**	**Challenges**
Lam Pham *et al*. [13]	Student-Teacher Scheme	Reduce model complexity substantially while maintaining very high accuracy.	Lack of standardized evaluation datasets
Faizan Karim *et al*. [14]	CNN	Improves the categorization problem accuracy	Reduce the likelihood of detection
Muhammad Umer *et al*. [15]	CNN	Accurately predict COVID-19 patients	Evaluation of the DL-based models' robustness and generalizability is very challenging.
Qiao Ke*et al.* [16]	Neuro-heuristic approach	Give the doctor decision support to make each case consultation faster and more accurate.	It's difficult to meet clinical needs for intelligent technologies.
Subrato Bharati *et al*. [17]	VGG Data STN	Simplify lung disease detection for both experts and medical professionals.	For rotated, slanted, or other abnormally oriented images, the fundamental CNN performs poorly.
Santosh Kumar *et al*. [18]	LSTM, CNN + SVM, and MLP	Encourages the use of health informatics that is built on accurate prediction, clinical decision, and early diagnosis	Identifying undiagnosed diseases is difficult
Ekram Chamseddine *et al.* [19]	SMOTE	Complete a multi-classification task that separates COVID-19, typical, and viral pneumonia cases.	The main issue is class imbalance
Anubhav Sharma *et al*. [20]	COVDC-Net approach	Improved overall classification accuracy	Overfitting

lung tissues in x-ray images, image descriptors depending on spatial distribution of hue, saturation, and brightness values in x-ray images were utilized, along with a NN working in conjunction with heuristic methods (Moth-Flame, Ant Lion). The proposed fitness function is used by NN to analyze the image, and if the probability of a respiratory illness is identified, the heuristic method specifically identifies the deteriorated tissues in the x-ray image.

In 2020, Subrato Bharati*et al*. [17] presented a novel hybrid deep learning architecture by merging VGG, data augmentation, and STN with CNN.Here, the new hybrid approach is known as VGG Data STN with CNN (VDSNet). A dataset of NIH chest X-ray images obtained from the Kaggle repository is used to test the proposed model. For rotated, slanted, or other abnormally oriented images, the fundamental CNN performs poorly.

In 2022, Santosh Kumar*et al*. [18] created a framework employing multimodal DL approaches for quick categorization and early diagnosis of COVID-19 symptoms. The suggested framework leverages the pre-trained network's selection method to choose the optimal fusion model from the pre-trained chest X-ray and cough models.

In 2022, Ekram Chamseddine *et al.* [19] created a reliable DL model that helps radiologists identify COVID-19 instances early by training on a balanced dataset. This work examined the WCL and subsequently the SMOTE on every dataset separately to solve the class imbalance problem. The models were created to carry out a multi classification task that separates instances of COVID-19, normal (no disease), and viral pneumonia.

In 2022, Anubhav Sharma*et al*. [20] have suggested a new hybrid CNN architecture that, with the aid of the confidence fusion method, combines the two distinct types of characteristics obtained from independent CNN architectures in order to better assist and diagnose COVID-19 patients.

The features and difficulties of the existing lung disease detection techniques are listed in Table 1.

B. Review

Some of the challenges related to lung disease detection faced in existing approaches are as follows: In Student-Teacher scheme [13] there is a lack of standardized evaluation datasets. CNN [14] decrease the likelihood of detection. Evaluation of the DL-based models' [15] robustness and generalizability are very challenging. It's difficult to meet clinical needs for intelligent technologies [16]. For rotated, slanted, or other abnormally oriented images, the fundamental CNN [17] performs poorly. Identifying undiagnosed diseases is difficult [18]. The main issue of SMOTE method [19] is class imbalance. In COVDC-Net approach [20], the main issue is overfitting.

And, the afore mentioned challenges like overfitting, and enhanced accuracy for unknown data are vanquish in the research work via incorporating the enhanced features set with pre-eminent features and fused features. Also, the model trained with the newly developed CBRACDC optimization for fine tuning the hyperparameter (i.e., weight) of the classifier in order to maximize the classifier's performance and diminish the predefined loss function to produce better results with less error.

3. Proposed Architecture for Lung Disease Classification with Multi-Modal Data.

As stated before, the proposed model introduces a new lung disease classification model via multi-modal data including text and X-ray images. The symptoms in the form of text are progressed along with the image data. Finally, the fused features from both the modality are subjected for final classification. Fig. 1 shows proposed lung disease classification model. Initially, the text and the image input are pre-processed in the pre-processing stage – data normalization is done for text data and image enhancement is performed for images.

After pre-processing, the subsequent step is the feature extraction and the text-based features and the image-based features are extracted – statistical features, IG, and improved entropy features are extracted from the pre-processed text data and GLCM, MBP and improved CSLBP features are extracted from the pre-processed image. Subsequently, feature fusion is carried out to fuse the text-based features and image-based features to extract the pre-eminent features which are passed as input to the last stage i.e., classification.

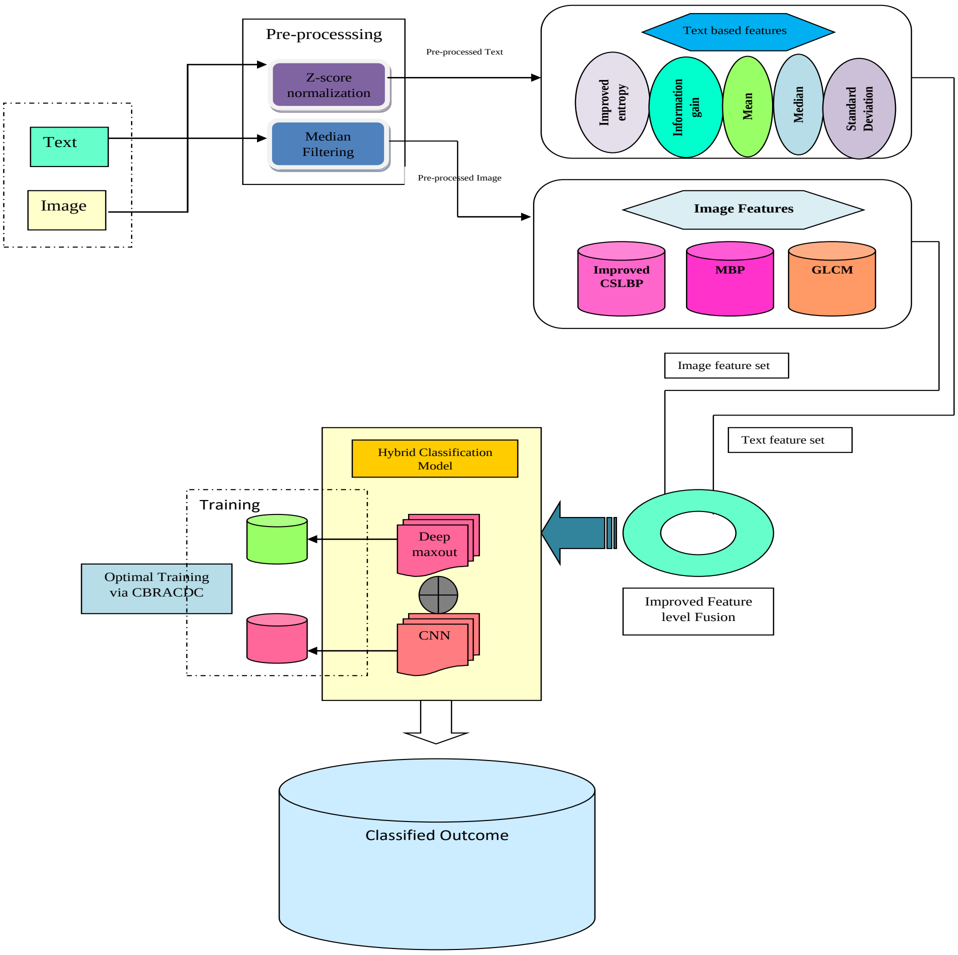

Fig 1. Overall layout of Lung Disease Detection from Multi-Model Data

As in classification, a hybrid classifier based on Deep Maxout and CNN is carried out. In addition, a novel customized battle Royale Optimization which is termed CBRACDC is used in the training process to enhance the performance of the classification in terms of accuracy and error.

4. Description of Pre-Processing, Feature Extraction, and Improved Feature Level Fusion

A. Preprocessing

In initial phase, both text and image will be carried out. Input text Ip^{Txt} is pre-processed by a data normalization technique. And input image Ip^{Ig} is pre-processed by an image enhancement technique.

For input text (Data normalization): In text pre-processing, data normalization will be done by Z-score normalization. Z-score normalization [21] is the process of transforming each value in a dataset so that the mean and standard deviation are both 0. Z-score normalization is done by applying the following formula (1) to each value in a dataset:

$$New_{value} = \frac{(a-\lambda)}{\sigma} \qquad (1)$$

Where, a is the real value, λ is the data mean, and σ is SD.

For input image (Image enhancement): In image pre-processing, image enhancement will be done by Median filtering. Utilizing the median filtering [22] technique, the input image is de-noised and smoothed. To create the digital image series as well as noise quantity, the neighbor mask of median value is also applied. The noisy value is replaced by an aggregated median value as well as the surrounding pixels, which are ordered by the grey scale. Here, $l(q,p) = mid\{K(q-y,p-x)y, x \in p\}$ denotes output of median filtering, whereas, 2D mask is denoted by p ,$H \times H$denotes size of mask, and $p(K,l)$,$l(q,p)$, denotes actual image & output of image. The mask's shape could be cross, square, circular, or linear.

B. Extraction of Text and Image Features: Multi-Modality

After pre-processing, the next step is feature extraction, which involves extracting features from the input text Ip^{Txt} and input image Ip^{Ig} .

For input text: Statistical features, information gain, and improved entropy features will be extracted from the input text. Extracted text feature is ex^{Tf} .

- **Statistical features**: Mean [23], Median [23], and SD [23] were the statistical features extracted from Ip^{Txt} .
- **IG:** A popular feature evaluation technique in the field of ML is called IG [24], which uses entropy. The term "IG" refers to the quantity of information provided by the feature items for the text category, which is used in the extraction of text feature information. The following equation (2) displays the IG formula:

$$M(O,r) = -\sum_{i=1}^{m} l(F_i)\, log\, l(F_i) + l(r)\sum_{i=1}^{m} l(F_i|r)\, log\, l(F_i|r) + l(\overline{r})\sum_{i=1}^{m} l(F_i|\overline{r})\, log\, l(F_i|\overline{r}) \quad (2)$$

Where, F is the collection of documents in which the feature r is not present. When $M(O,r)$ has a higher value, r is more helpful in categorizing F . It is best to choose this r . $l(r)$ and $l(\overline{r})$ value should be decreased if a higher value of $M(O,r)$ is desired.

- **Improved entropy**: An indicator of the degree of uncertainty around random variables is entropy. Conventional entropy formula is given in eq. (3)

$$T(U) = Q = -\sum_{i=1}^{n} z(u_i) * \log_2(z(u_i)) \qquad (3)$$

As per improved concept, improved entropy formula is given in eq. (4)

$$T(U) = Q = -\sum_{i=1}^{n} \frac{z(u_i) * \log_2(z(u_i))}{2^{|B|}-1} \qquad (4)$$

Where, $T(U)$ is the uncertainty of U , $z(u_i)$ is the probability with result u_i , and $|B|$ defines the cardinality of u_i . Cardinality is the element count in a set.

For input image: Texture features like GLCM, MBP, and Improved CSLBP features will be extracted from the input image. Extracted image feature is denoted as ex^{If} .

- **GLCM**: [25] A pixel a of grey intensity and a pixel b of grey intensity are separated by a ϑ translation vector that is determined by the direction and a distance c , and these probabilities $prob^{(a,b,c,\vartheta)}$ are represented by GLCM. Where c depicts distance among 2 pixels and ϑ depicts angle among 2 pixels. GLCM is described mathematically in eq. (5).

$$prob^{(a,b,c,\vartheta)} = \Phi\left\{ \begin{array}{l} (p1,q1)(p2,q2) \mid i(p1,q1) = a, i(p2,q2) = b, |(p1,q1) \\ -(p2,q2)| = c, \angle((p1,q1),(p2,q2)) = \vartheta \end{array} \right\} \qquad (5)$$

Where, Φ denotes the occurrence frequency inside the window, a and b are the first and second pixels' respective gray scale intensities at positions $(p1, q1)$ and $(p2, q2)$, correspondingly.

- **MBP**: Rather than always employing the centre pixel, the MBP operator thresholds the pixels over their median within a neighborhood to map from intensity region to an LBP [26]. In equation (6), MBP in pixel (s, t) is given:

$$MBP(s,t) = \sum_{q=0}^{Z-1} 2^q J(g_q - \lambda) \quad (6)$$

Where, z is the size of patch, λ is the threshold value, g represents the binary bits, and λ displays the median calculated over the local patch.

- **Improved CSLBP**: The CSLBP [27] operator analyzes centre symmetric pairings of nearby pixels as a modified version of the popular LBP operator. The formal representation of traditional CS-LBP is eq. (7).

$$CSLBP_{J,K}(m,n) = R = \sum_{i=0}^{(K/2)-1} t\left(k_i - k_{i+(K/2)}\right).2^i \quad (7)$$

Here $t(a) = \begin{cases} 1, a > V \\ 0, otherwise \end{cases}$

Where, k_i and $k_{i+(K/2)}$ relates to the gray levels of the centre symmetric pairings of pixels of K pixels with equal spacing around a circle with a radius J.

According to improved concept, CSLBP is represented as per eq. (8)

$$CSLBP_{J,N}(m,n) = R = \sum_{i=0}^{(K/2)-1} \frac{t\left(k_i - k_{i+(K/2)}\right).2^i}{I} \quad (8)$$

Where, I is the Soblel edge detection calculated as per eq. (9).

$$I = \sqrt{Iu^2 + Iv^2} \quad (9)$$

Here, Iu is the u directional kernel *(3×3 image portion having (u, v) as center cell), and Iv is the v directional kernel *(3×3 image portion having (u, v) as center cell).

C. Steps followed in improved feature level fusion

From the extracted feature ex^{Tf} and ex^{If}, improved feature level fusion will be done. The procedures used for improved feature level fusion are as follows:

- Using an improved entropy approach (Q), obtain the normalized text feature.
- Utilizing an improved CSLBP approach (R), acquire the feature of a normalized image.
- Manhattan distance (MH) among sample Q and R was computed as per formula (10).

$$MH(m,n) = |Q_1 - Q_2| + |R_1 - R_2| \quad (10)$$

Here, $m = (q_1, q_2, ...q_n)$ and $n = (r_1, r_2, ...r_n)$

Where, m, n refers distance among 2 points.

- Save the matrix's column width.
- Create vectors with linear spacing among 0 and 1 columns (L).
- Apply the Kronecker product merging, then save the results in eq. (11).

$$W = (Q \otimes L)MH + R \otimes (1 - L)) \times xx_i \quad (11)$$

Where, xx_i is the weight function estimated using the chebyshev map in eq. (12).

$$M_{K+1} = \cos(0.5 \cos^{-1} M_K) \quad (12)$$

5. Hybrid Classification: Averaging Deep Maxout and Cnn

The fused features from the previous step is subjected for hybrid classification model, where the lung diseases are classified [28] A hybrid classifier combining CNN and Deep Maxout classifiers is used in this step. To increase the performance of the classification findings, a novel CBRACDC algorithm will be utilized to train the hybrid model, which is briefly detailed in the following section. The proposed hybrid classification model is shown in Fig. 2.

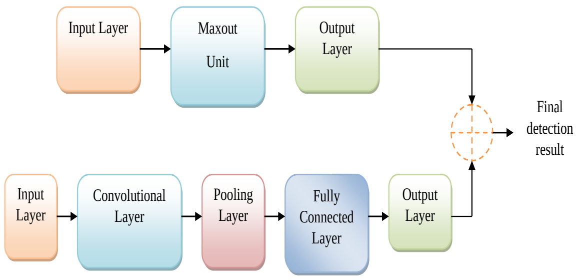

Fig 2. Hybrid process (Averaging Deep Maxout and CNN)

A. Optimized Deep Maxout

In a Maxout NN [29], each neuron is a member of a collection of f candidate items. It was decided to use a max value extending f elements for neuron activation. The i^{th} node of the a^{th} hidden layer should be represented as D_a^i, and its constituent parts as K_a^{ij}. Equations (13) and (14) provide a satisfying connection between them: K_a^{ij} is obtained through the forward propagation of a layer below:

$$D_a^i = \max_{j \in 1,2,\ldots,f} K_a^{ij} \qquad (13)$$

$$K_a = Q^{*Z}_{a-1} D_{a-1} + e_a \qquad (14)$$

Here, $D_{a-1} \in J^I$ is a $a-1$ layer's max-out activation vector, $Q^*_{a-1} \in J^{I \times K}$ is a $a-1$ layer's weight matrix which is tuned optimally by proposed CBRACDC method, $K_1 \in J^K$ is a a^{th} layer vector, and $e_a \in J^K$ is a a^{th} layer's bias vector. Owing to the activation computations, the forward-propagation procedure of the maxout network is different comparing with conventional feed-forward NN. In back propagation $\{K_a^{ij} \mid j \in 1,\ldots, f\}$ for $i \in [1, N^a]$, $a \in [1, A]$, no additional weights are employed; only those connected to the element that occurs the majority of the time inside each group, and its training implementation is always 1 for all maxout neurons. It is the same as convolutional networks' max-pooling. Convolutional networks, in contrast to maxout networks, show max-pooling over spatial position. The concept of max-pooling across f pieces is the distribution of distinctive features throughout a specified geographic area.

B. Optimized CNN

CNN [30] is the most popular ANN type for evaluating visual input. In CNN, various layer types were applied. CNN weight sharing feature decreases the number of learnable parameters inside the network, which is one of the primary reasons to use it in this situation because it helped the network to avoid overfitting and increase generalization. CNN weight is denoted as Q^{**}.

Rectification layer: Rectification layer is said to be a Layer ll. Subsequently, its input consists of o_1^{ll-1} feature maps with a size of $o_2^{ll-1} \times o_3^{ll-1}$. Equation (15) is used to determine the absolute value of each feature map:

$$P_i^{ll} = \mid P_i^{ll} \mid \qquad (15)$$

Convolutional Layer: The most crucial element of any CNN architecture is the convolutional layer. Convolutional layer is said to be a layer ll. The next step is to add the feature mappings o_1^{ll-1} from the input layer ll of the preceding layer, with a size of $o_2^{ll-1} \times o_3^{ll-1}$. If $ll = 1$, there is only one source data X, it could have one or even more channels. Layer ll output consists of o_1^{ll} feature maps with a size of $o_2^{ll} \times o_3^{ll}$. The ll layer's i^{th} feature map was represented by the P_i^{ll} symbol, which was stated in an equation (16). Where, $M_{i,j}^{ll}$ is referred as a filter, and F_i^{ll} is referred as a bias matrix.

$$P_i^{ll} = F_i^{ll} + \sum_{j=1}^{o_1^{ll-1}} M_{i,j}^{ll} * P_j^{ll-1} \qquad (16)$$

Pooling layer: The feature maps are sub-sampled using pooling layers. Layer ll is said to be a pooling layer. Reduced-size $o_1^{ll} = o_1^{ll-1}$ feature maps are the outcome of this algorithm. Windows are typically positioned at non-overlapping points within each feature map while preserving one value for each window in order to subsample all feature maps.

Pooling layer's primary disadvantage is that it regularly makes CNN perform worse. The reason for this is that the pooling layer enables CNN to determine if a particular feature is present in the input image or not without worrying about the feature's exact location.

FC Layer: Typically, the last layer of CNN architecture is made up of FC layers, where each layer's neurons are linked to those of the layer before it. The CNN design uses the final FC layer as the output layer. Layer ll is said to be a FC layer. The i^{th} unit in Layer ll is generated according to eq. (17), and Layer ll anticipates receiving o_1^{ll-1} feature maps with size $o_2^{ll-1} \times o_3^{ll-1}$ as input.

$$P_i^{ll} = h(c_i^{ll}) \qquad (17)$$

6. Customized Battle Royale Algorithm with Canberra Distance Calculation (Cbracdc)

A. **Objective function and solution encoding**

The classification accuracy is highly relying on the minimization of error, i.e, the error between actual and predicted value. As per the work, the error minimization is fixed as the objective while tuning the optimal weights as depicted in figure 3. The mathematical modeling of the defined objective function is defined in Eq. (18).

$$oBj = \min(error) \qquad (18)$$

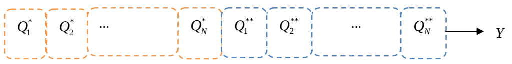

Fig. 3. Solution encoding

Here we introduce a new CBRACDC method which is used to train hybrid model (Deep maxout and CNN) in order to enhance performance of classification results. It is observed that the self-improved optimization concept may enhance the convergence rate and speed on solving the given optimization issue rather than the traditional procedure. Hence, we customized the battle royale optimization assisting with new distance evaluation for position update.

Our proposed algorithm procedure is as follows: Random population is evenly distributed across the problem space is the starting point for BRO [31]. Each soldier then fires a weapon in an effort to injure the one who is closest to them. Consequently, soldiers in best positions harm their immediate neighbours'. Each time a soldier is injured by another, the damage level goes up by one. Such interactions are calculated mathematically according to . Where, is the degree of the soldier's damage among the population. Also, Soldiers prefer to shift positions as soon as they sustain damage, so they attack enemies from other side. As a result, in order to concentrate on exploitation, the damaged solder travels in the direction of a position midway between its original location and the best position so far. According to equation (19), these exchanges are mathematically calculated:

$$Y_{dmg,f} = Y_{dmg,f} + h\left(Y_{best,f} - Y_{dmg,f}\right) \quad (19)$$

Where, is damaged soldier location in dimension , is a randomized value. As per the proposed logic, randomization is evaluated using the logistic map function given in eq. (20).

$$B_{l+1} = 4B_l(1.B_l) \quad (20)$$

If the wounded soldiers will be able to harm the opposing team in the following round, then was reset as zero. Additionally, in order to concentrate on exploration, a soldier dies and respawns randomly from a feasible problem space if their damage level exceeds a certain threshold number, and would reset as zero. Herethreshold value is 3 which were suitable after plenty of trial and error. Better exploration is made possible by avoiding early convergence. After being killed, the soldier returns to the problem space as shown in equation (21):

$$Y_{dmg,f} = h(Up_f - Lw_f) + Lw_d \quad (21)$$

Where, , is the upper and lower bounds of dimension in problem space, respectively.

According to proposed CBRACDC approach, new position update of soldier is given in eq. (22)

$$Y_{dmg,f} = \frac{h(Up_f - Lw_f) + Lw_f}{CanD} \quad (22)$$

Where is a Canberra distance which is a quantitative way to express the distances between two vector space point pairs. Additionally, at each iteration , the problem's feasible search space starts to contract in the direction of the ideal resolution[33]. The starting value was but then . Here is the number of generations at their maximum. Exploration and exploitation are both aided by this connection. Therefore, eq. (23) will update the lower and upper bound:

$$lb_d = x_{best,d} - SD\left(\overline{x_d}\right), Up_f = Y_{best,f} + SD\left(\overline{Y_f}\right) \quad (23)$$

Where, $SD\left(\overline{Y_f}\right)$ refers SD of entire population in dimension f , and $Y_{best,f}$ is the location of best solution so far. As a result, the Lw_f / Up_f sets to an actual Lw_f / Up_f if it crosses the actual lower/upper bound. In order to emphasize elitism, the top player or soldier from each iteration is retained and regarded as elite[34]. Aside from the problem's dimensions, the proposed approaches computing cost also dependent on the size of the population and maximum allowed iterations. Considering a population size , the complexity of computing for all solutions is $O(t^2)$ as every solution must be contrasted to all other solutions in order to determine its Euclidean distance from every other solution. Therefore, given iterations, BRO's computational complexity is $O(s^3)$. The pseudocode of proposed CBRACDC method is given in Algorithm 1:

Algorithm 1: Customized Battle Royale Algorithm with Canberra Distance Calculation (CBRACDC)
Begin
Initialize entire parameters
$shrink = ceil(\log_{10}(Max\_Cicle))$
$\nabla = round(Max\_Cicle / shrink)$
$iter = 0;$

While termination condition is not reached do
$iter = iter + 1$
for $i = 1 : pop^{Size}$
$dmg = j$
$vic = i$
if $w(Y_i) < w(Y_j)$
$dmg = i$
$vic = j$
end if
if $x_{dmg}.damage < Threshold$
for $d = 1 : Dimension$
Damaged soldier's position will be changed depending on: $Y_{dmg,f} = h(max(Y_{dmg,f}, Y_{best,f}) - min(Y_{dmg,f}, Y_{best,f})) + max(Y_{dmg,f}, Y_{best,f})$
According to proposed CBRACDC approach randomness h in eq. (19) is estimated using Logistic map function.
end for f
$Y_{dmg}.damage = Y_i.damage + 1$
$Y_{vic}.damage = 0$
else
for $f = 1 : Dimension$
Position update of soldier is calculated as per eq. (22) according to proposed CBRACDC approach.
End for f
Update $w(Y_{dmg})$
$Y_{dmg}.damage = 0$
end for i
if $iter >= \nabla$
update $(Up - Lw)$ depending on equation (23)
$\nabla = \nabla + round\left(\frac{\nabla}{2}\right)$
end if
if the Lw_f / Up_f extends actual $lower / upper$ bound then set it to real Lw_f / Up_f
end if

end while
Choose best soldier as result

7. Results and Discussion

A. Simulation Procedure

Python was used to execute this proposed Customized Battle Royale Algorithm with Canberra Distance Calculation (CBRACDC) model for Lung Diseases Classification. The assessment on proposed model is done over the conventional classifiers including Blue Monkey Optimization (BMO), Moth Flame Optimization (MFO), Shuffled Shepherd Optimization (SSO), Spider Monkey Optimization (SMO) and Battle Royale Optimization (BRO). The performance of the proposed model had been evaluated in terms of Accuracy, FNR, Precision, MCC, FPR, F-measure and so on. Accuracy, F-measure, sensitivity, and other positive metrics should be maximized, while the negative measures (FNR, FPR), should be minimized, for acceptable results. Table II illustrates the sample count for various learning percentage.

Table II. Sample count for various learning percentages

Learning percentage – 60%	
Training	1354
Testing	904
Learning percentage – 70%	
Training	1580
Testing	678
Learning percentage – 80%	
Training	1806
Testing	452
Learning percentage – 90%	
Training	2032
Testing	226

B. Dataset Description

Moreover, the dataset was collected manually. Here, the total images used in dataset were 2286×3600 images. Further, the classified eight chest diseases includes atypical chest pain, bronchial asthma, GERD, MI, panic attack, pneumonia, stable angina, and URTI which has similar presentation. Further, the atypical chest pain includes 350 images, the bronchial asthma includes 208 images, the GERD includes 400 images, the MI includes 84 images, the panic attack includes 141 images, the pneumonia includes 608 images, the stable angina includes 117 images, and the URTI includes 380 images. For 80% of learning, the training consists of 2057 images and training includes 229 images. In addition, the training consists of 1828 images and testing includes 458 images for 70% of learning. For 60% of learning, the training consists of 1600 images and training includes 686 images. Likewise, the training consists of 1371 images and training includes 915 images for 50% of learning. Along with this, the symptoms of the corresponding diseases are also specified.

C. Analysis on Positive measure

The positive measure (Accuracy, Sensitivity, Precision and Specificity) are examined for the proposed CBRACDC model and for the current methods. Fig 4 illustrates the overall performance evaluation of all the classifiers. Additionally, it is determined by changing the learning percentage to 60, 70, 80 and 90. The majority of classifiers exhibit the greatest improvement as the learning percentage rises. Nevertheless, the suggested method has produced the outcomes with high classification accuracy, sensitivity, precision and specificity. This indicates the effective of the proposed work for categorizing the lung diseases. For all learning percentages, the BMO and BRO strategy exhibits the poorest performance with low classification accuracy. In fig 4(a), the accuracy attained using proposed method is very high (95.28%), than the compared methodologies such as BMO (81.42%), BRO (83.44%), SSO (82.19%) and SMO (83.44%), at the 90% of learning rate.

Additionally, while reviewing the fig 4(b), 4(c), the specificity and precision should be greater for the excellent approach. Likewise, the proposed model recorded the higher precision and specificity over BMO, BRO, SSO and SMO. In the final (90%) learning percentage, the precision and specificity of the suggested model is 96.83% and 78.96%.

The proposed method obviously outperformed previous methods for classifying lung disease, and the results are considerably improved. Similar to fig. 4(c), the suggested strategy achieved above (~) 90% of sensitivity, surpassing the other existing methods in the entire learning rate. The proposed method offered the maximum precision at 92.48%, 94.09%, 96.35%, and 97.83% for the learning rates of 60%, 70%, 80%, and 90%, respectively. Therefore, it is obvious from the evaluation that the proposed CBRACDC based model is significantly more effective for classifying the lung diseases with high accuracy and precision rate. This enhancement is mainly rely with the assistance of optimal training that makes the model to categorize accurately by minimizing the error.

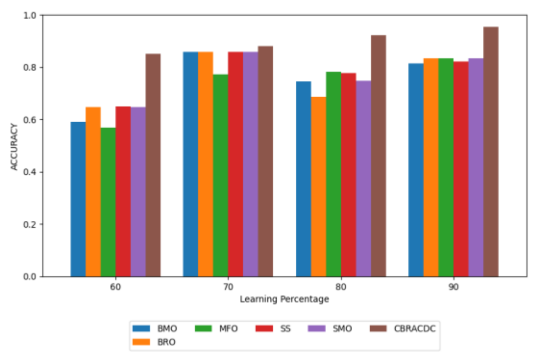

Fig 4 (a) proposed CBRACDC model performance Accuracy

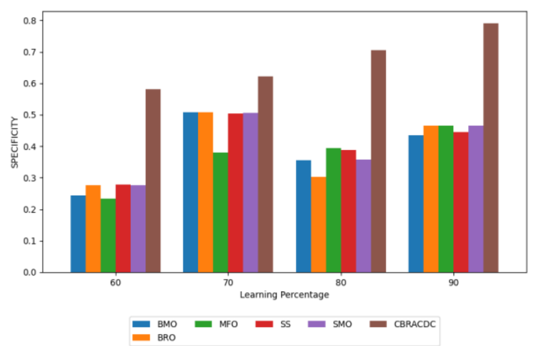

Fig 4 (b) proposed CBRACDC model performance Specificity

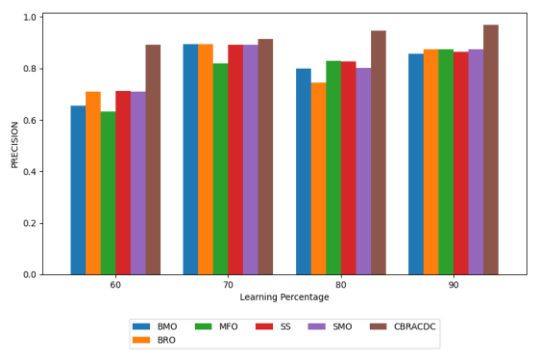

Fig4 (C) proposed CBRACDC model performance Precision

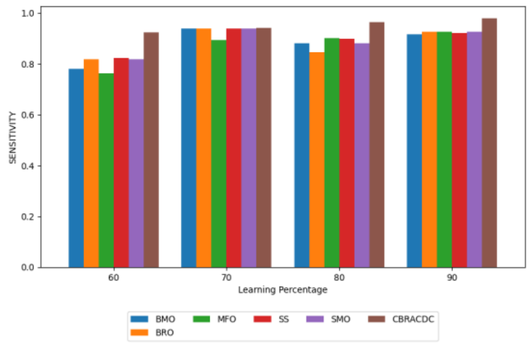

Fig 4 (d) proposed CBRACDC model performance Sensitivity

D. Analysis on Negative measure

Comparative study of the proposed CBRACDC model with the existing models in terms of negative measure (FNR, FPR) is shown in Fig. 5. The FNR and FPR of the proposed work are reduced as the learning percentage progressively rises. Likewise, compared to other existing methodologies, the proposed model lowered the error rate. When results are defined in terms of FPR at 60% learning rate, the suggested model secured a low FPR of 0.419561 as contrasting to BMO is 0.756029, BRO is 0.724014, MFO is 0.76657, SSO is 0.721226 and SMO is 0.419561. Similar to this, BMO and SSO have the highest FPR (0.584551 and 0.554551), meanwhile the suggested methodology barely succeeded in achieving the FPR of 0.210315.

The proposed work has produced an extraordinary outcome when seen in the context of FPR metric, namely that it is less error-prone in the entire learning percentage. Additionally, the FPR of the suggested model at the 80% of learning percent is 0.036446, which is incredibly low in comparison to the established approaches, such as BMO=0.118942, BRO=0.154999, MFO=0.098874, SSO=0.101333, and SMO=0.11766. Experimental outcomes prove that the proposed CBRACDC technique performs superbly for identifying as well as classifying the lung diseases.

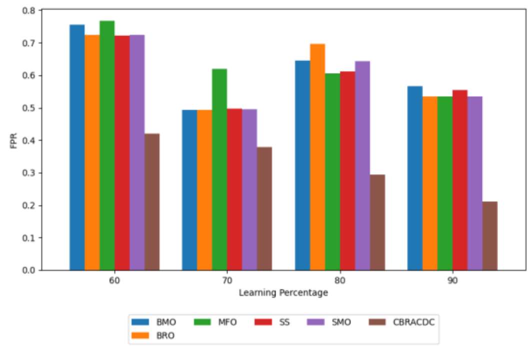

Fig 5 (a) the proposed CBRACDC model performance FPR

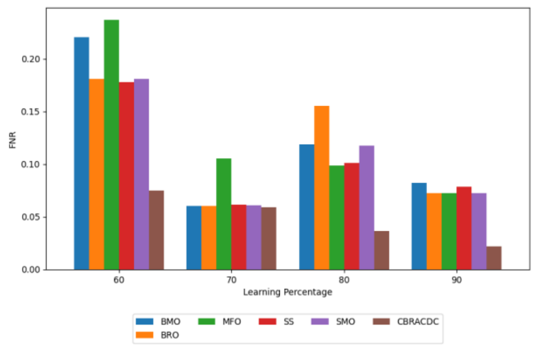

Fig 5 (b) the proposed CBRACDC model performance FNR

E. **Analysis on Other measure**

We evaluate the other measures to get greater credibility for the proposed model. The suggested CBRACDC model's other measure is higher than those of the current techniques then it is perfectly appropriate for the categorization of lung disorders. Additionally, despite variations in the learning percentage, the suggested methodology still yielded the highest value across all metrics. Fig. 6 provides an illustration of other measure for the suggested model compared to the conventional models. The adopted model's F-measure, which is greater than that of the BMO, MFO, SSO, SMO, and BRO, is 97.29% at the 90% learning percentage. The MCC of the adopted strategy is 53.55% (at a learning percentage of 60%), and it further enhances to 79.26% in the final learning percentage. This illustrates that the proposed model MCC's is raised by an increase in the learning percentage.

Additionally, NPV analysis has been done, the NPV of the suggested method at learning percentages of 60, 70, 80, and 90, respectively, is 67.70%, 71.38%, 78.45%, and 85.05%. As a conclusion, the suggested CBRACDC classifier performs better since it can consistently classify the lung disease more accurately.

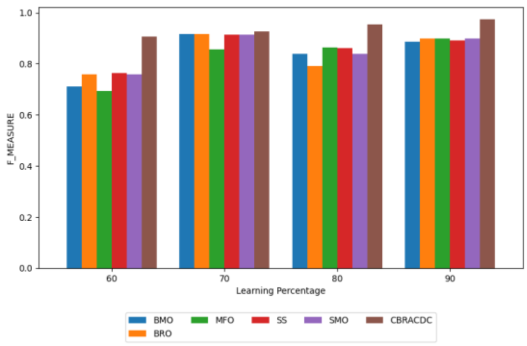

Fig 6 (a) the proposed CBRACDC model performance F-measure

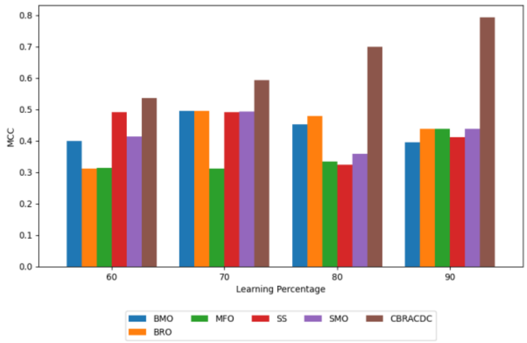

Fig 6 (b) the proposed CBRACDC model performance MCC

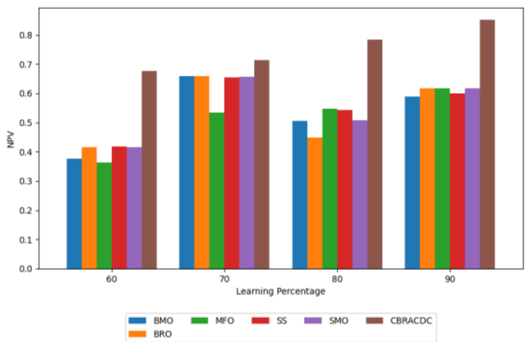

Fig 6 (c) the proposed CBRACDC model performance NPV

F. Ablation Study

Nine distinct measures, including Accuracy, F-measure, FPR, and other measures, are used to assess the ablation study. Also, the proposed method is compared against model without optimization, model with conventional entropy and model with conventional CSLBP. Table III exhibits a comparison of the adopted approach to the other features. Particularly, the classification accuracy obtained by the proposed work is 95.28%, model with conventional entropy is 81.75%, model with conventional CSLBP is 81.83% and model without optimization is 75.29%. Additionally, the FPR secured by the model with conventional entropy, model with conventional CSLBP, model without optimization and proposed model is 0.152721, 0.15246, 0.16906 and 0.210315, respectively.

Similarly, the F-measure, FNR, precision of the proposed method is 97.29%, 0.021656 and 96.75%. The sensitivity of the proposed method (97.83%), model with conventional entropy (80.66%), model with conventional CSLBP (80.77%) and model without optimization (71.52%). Altogether, it is observed that the model with conventional strategies or logics degrades the performance with least accuracy, and the proposed model with all the enhancement and optimal training drastically increases the accuracy rate. This shows the significance of optimal training with further feature level enhancement in classifying the diseases.

.

TABLE III. ABLATION STUDY

	Proposed with conventional entropy	Proposed with conventional center symmetric LBP (CSLBP)	Proposed without optimization	CBRACDC
Accuracy	0.81751	0.81835	0.752948	0.952875
Sensitivity	0.806689	0.807782	0.71522	0.978344
Specificity	0.847279	0.84754	0.83094	0.789685
Precision	0.935614	0.936036	0.897388	0.967538
F-measure	0.866381	0.867192	0.796015	0.972911
MCC	0.59973	0.600842	0.513453	0.792663
NPV	0.614377	0.614855	0.585317	0.850549
FPR	0.152721	0.15246	0.16906	0.210315
FNR	0.193311	0.192218	0.28478	0.021656

G. Statistical Analysis with respect to Error

Despite its stochastic nature, optimization is routinely employed to produce outcomes that can be validated using statistical measurements. The five various case scenarios, such as Minimum, Mean, Maximum, Standard Deviation, and Median, are used to examine the suggested approach and the existing models. The statistical study is tabulated in table IV. Analysis of the table revealed that the suggested CBRACDC strategy has lower error than the existing approaches. In the mean case scenario, the suggested technique obtain the error rate as 1.05564, that is relatively low as compared to the other approaches like BMO is 1.07422, BRO is 1.064, MFO is 1.05799, SSO is 1.06652 and SMO is 1.06107, respectively. In addition, existing methodologies like BMO=1.07529, BRO=1.06515, MFO=1.05952, SSO=1.06314, and SMO=1.05883 obtain the highest error value in the median case scenario, but even the suggested approach yields the errorrate as 1.05273.

Furthermore, in the minimum case scenario analysis, the suggested work error value is 1.04973, which is noticeably better than the extant models like BMO (1.06291), BRO (1.06276), MFO (1.0557), SSO (1.06314) and SMO (1.05883).

TABLE.IV STATISTICAL ANALYSIS WITH RESPECT TO ERROR.

	BMO	BRO	MFO	SSO	SMO	CBRACDC
Mean	1.07422	1.064	1.05799	1.06652	1.06107	1.05564
Median	1.07529	1.06515	1.05952	1.06314	1.05883	1.05273

Standard Deviation	0.007496	0.001194	0.001869	0.004834	0.00253	0.0068
Minimum	1.06291	1.06276	1.0557	1.06014	1.05883	1.04973
Maximum	1.08129	1.06515	1.05952	1.07143	1.06392	1.06537

H. Analysis on Classifiers

Table V provides illustrations of various classifiers are compared using the various metric categories. Again, the suggested CBRACDC+hybrid classifier yielded the best classification accuracy while lowering the error rate. The Maxout (92.79% of accuracy) and AHGOA (93.23% of accuracy) have similar results as the suggested method. However, the proposed model has 95.28% accuracy rate, which is greatest. Similarly, the suggested work achieves the lowest FNR of 0.021656 that is superior to CNN is 0.087902, DCNN is 0.050102, DBN is 0.25967, RNN is 0.144011, SVM is 0.065587 and Maxout is 0.056696, respectively.

In the examination of F-measure, the suggested model recorded the F-measure of 97.29%, although the AHGOA and DBN algorithm obtained the lowest F-measures of 72.92% and 80.81%, respectively. Consequently, when compared to existing approaches, the proposed work has higher levels of sensitivity, specificity, and precision. According to the study of all classifier comparisons, the DBN technique exhibited the worst performance, while the proposed model seemed to have the best performance. Thereby, the proposed hybrid classification with the proposed training algorithm shows its drastic performance on solving the classification problem with better error rate to yield high accuracy rate.

I. Convergence Analysis

In order to evaluate the convergence study we have compared our proposed CBRACDC method over the conventional models (BMO, MFO, SMO, BRO and S-S), and the output graph is given in figure 7. The analysis is carried out by changing the iterations to 5, 10, 15, 20 and 25, respectively. For optimal system performance, the presented work must attain least error rate. The suggested model initially exhibits a slightly higher error value from iteration 0 to iteration 8, but from iteration 9-15, the proposed model shows a comparatively minimal error rate than the value reached between iteration 0 to 8. At last, the minimal error rate of 1.0501 is reached at the final iterations 16–25. Error rates of 1.0579, 1.0598, and 1.0625 are attained by the MFO, SMO, and SSO, respectively (in the 50th iteration). Thereby, it is clearly proven that the proposed CBRACDC strategy has been improved for lung disease classification with reduced error.

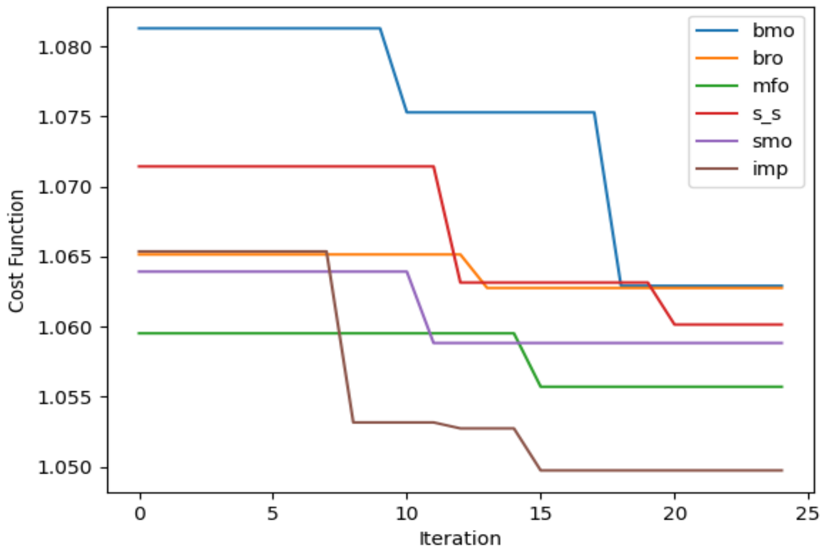

Fig 7. Convergence analysis between the proposed CBRACDC model and conventional approaches

Table V. Analysis on Classifiers

	CNN	DCNN[32]	DBN	RNN	SVM	MAXOUT	AHGOA [33]	CBRACDC+Hybrid Classifier
Accuracy	0.903328	0.924596	0.742977	0.844376	0.916879	0.927918	0.932314	0.952875
Sensitivity	0.912098	0.949898	0.740321	0.855989	0.934413	0.943304	0.729258	0.978344
Specificity	0.865325	0.9008	0.750205	0.798392	0.834138	0.871085	0.961323	0.789685
Precision	0.967049	0.981694	0.889668	0.943858	0.963749	0.964322	0.729259	0.967538
F-measure	0.93877	0.965534	0.808153	0.897779	0.948854	0.953697	0.729259	0.972911
MCC	0.717067	0.795664	0.445529	0.587365	0.729859	0.792142	0.69058	0.792663
NPV	0.694348	0.762497	0.514991	0.583354	0.729367	0.806181	0.961237	0.850549
FPR	0.234675	0.2992	0.249795	0.221608	0.265862	0.228915	0.038678	0.210315
FNR	0.087902	0.050102	0.259679	0.144011	0.065587	0.056696	0.270742	0.021656

8. Conclusion

Our research goal is to build a new Lung Disease Classification from Multi-model data, especially text (symptoms) and X-ray images. As a result, the suggested model includes a number of steps, including pre-processing, feature extraction, feature level fusion, and classification. The initial stage is where the text and image preprocessing will take place. Data normalization is done for text, while image enhancement is done for input image. Feature extraction, which comes after preprocessing, entails extracting features from the input text and image. Statistical features, IG, and improved entropy features will be extracted from the input text. GLCM, MBP, and Improved CSLBP features would be extracted from the input image. In, improved feature level fusion, the text-based features and the image-based features are fused. By combining models like Deep Maxout and CNN, a hybrid classifier will be created to categorize lung diseases. In order to train the hybrid model more effectively and produce better classification outcomes, a novel CBRACDC will be suggested. Finally, the effectiveness of the recommended algorithm was assessed, and the result was effectively verified.

References

[1] Remco de Kock, Ben van den Borne, Maggy Youssef- El Soud, Huub Belderbos, Gerben Stege, Marleen de Saegher, Claartje van Dongen-Schrover, Sylvia Genet, Luc Brunsveld, Volkher Scharnhorst, Birgit Deiman, "Circulating biomarkers for monitoring therapy response and detection of disease progression in lung cancer patients ", 2021.

[2] Inaki Salvador-Corres,a Bibiana Quirant-Sanchez, Aina Teniente-Serra, Carmen Centeno, Amalia Moreno, Laura Rodríguez-Pons,Pere Serra-Mitjá, Marian García-Nunez, Eva Martinez-Caceres, Antoni Rosell, Alejandro Olivé, Karina Portillo, "Detection of autoantibodies in bronchoalveolar lavage in patients with diffuse interstitial lung disease", Archivos De Bronconeumologia, 2021.

[3] Cameli. P, Plataroti. D, Rana. G.D, Bergantini. L, Alessandro. M, Bargagli.E, "Serial autoantibody detection in interstitial lung diseases: should they be repeated at follow-up?", Pulmonology Volume 27, Issue 3, May–June 2021

[4] Bei Liu, Huiqing Yu, Xiaoping Zeng, Dan Zhang, Juan Gong, Ling Tian, Junhui Qian, Leilei Zhao, Shuya Zhang, Ran Liu, "Lung cancer detection via breath by electronic nose enhanced with a sparse group feature selection approach", Sensors and Actuators B: Chemical Volume 339, 15 July 2021.

[5] Dina M. Ibrahim, Nada M. Elshennawy, Amany M. Sarhan, "Deep-chest: Multi-classification deep learning model for diagnosing COVID-19, pneumonia, and lung cancer chest diseases", Computers in Biology and Medicine, 2021.

[6] Christie Emsley, Susannah King, Ibolya Nyulasi, Gregory Snell, "A GLIMmer of insight into lung transplant nutrition: Enhanced detection of malnutrition in lung transplant patients using the GLIM criteria", clinical nutrition, Volume 40, Issue 5, May 2021.

[7] Laxmikant Tiwari, Rohit Raja, Vineet Awasthi, Rohit Miri, G.R. Sinha, Monagi H. Alkinani, Kemal Polat, "Detection of lung nodule and cancer using novel Mask-3 FCM and TWEDLNN algorithms", Measurement, 2021.

[8] Mohsen Salimi, Seyed Mohammad Reza Milani Hosseini, "Smartphone-based detection of lung cancer-related volatile organic compounds (VOCs) using rapid synthesized ZnO nanosheet ", Sensors and Actuators: B. Chemical, 2021.

[9] Ruchita Shandilya, Shashi Ranjan, Surbhi Khare, Arpit Bhargava, Irina Yu Goryacheva and Pradyumna Kumar Mishra, "Point-of-care diagnostics approaches for detection of lung cancer associated circulating miRNAs", Drug Discovery Today, Volume 26, Issue 6, June 2021.

[10] Salehe Erfanian Ebadi, Deepa Krishnaswamy, Seyed Ehsan Seyed Bolouri, Dornoosh Zonoobi, Russell Greiner, Nathaniel Meuser-Herr, Jacob L. Jaremko, Jeevesh Kapur, Michelle Noga, Kumaradevan

Punithakumar, "Automated detection of pneumonia in lung ultrasound using deep video classification for COVID-19", Informatics in Medicine Unlocked, 2021.

[11] Prasad Dutande, Ujjwal Baid, Sanjay Talbar, "LNCDS: A 2D-3D cascaded CNN approach for lung nodule classification, detection and segmentation", Biomedical Signal Processing and Control, 2021.

[12] Diane M Gray, Sandra Kwarteng Owusu, Marieke M van der Zalm, "Chronic Lung Disease in Children: disease focused use of lung function", Current Opinion in Physiology, 2020.

[13] L. Pham, H. Phan, R. Palaniappan, A. Mertins and I. McLoughlin, "CNN-MoE Based Framework for Classification of Respiratory Anomalies and Lung Disease Detection," in IEEE Journal of Biomedical and Health Informatics, vol. 25, no. 8, pp. 2938-2947, Aug. 2021, doi: 10.1109/JBHI.2021.3064237.

[14] Faizan Karim, Munam Ali Shah, Hasan Ali Khattak, Zoobia Ameer, Umar Shoaib, Hafiz Tayyab Rauf, Fadi Al-Turjman, "Towards an effective model for lung disease classification Using Dense Capsule Nets for early classification of lung diseases", Applied Soft Computing, 2022.

[15] Umer, M., Ashraf, I., Ullah, S. et al. COVINet: a convolutional neural network approach for predicting COVID-19 from chest X-ray images. J Ambient Intell Human Comput 13, 535–547 (2022). https://doi.org/10.1007/s12652-021-02917-3.

[16] Qiao Ke, Jiangshe Zhang, Wei Wei, Dawid Połap, Marcin Wo ´zniak, Leon Ko ´smider, Robertas Damaševi ˇcius, "A neuro-heuristic approach for recognition of lung diseases from X-ray images", Expert Systems With Applications, 2020.

[17] Subrato Bharati, Prajoy Podder, M. Rubaiyat Hossain Mondal, "Hybrid deep learning for detecting lung diseases from X-ray images", Informatics in Medicine Unlocked, 2020.C.

[18] Santosh Kumar, Mithilesh KumarChaube, Saeed Hamood Alsamhi, Sachin Kumar Gupta, Mohsen Guizani, Raffaele Gravina, Giancarlo Fortino, "A novel multimodal fusion framework for early diagnosis and accurate classification of COVID-19 patients using X-ray images and speech signal processing techniques", Computer Methods and Programs in Biomedicine, 2022.

[19] Ekram Chamseddine, Nesrine Mansouri, Makram Soui, Mourad Abed, "Handling class imbalance in COVID-19 chest X-ray images classification: Using SMOTE and weighted loss", Applied Soft Computing, 2022.

[20] Anubhav Sharma, Karamjeet Singh, Deepika Koundal, "A novel fusion based convolutional neural network approach for classification of COVID-19 from chest X-ray images', Biomedical Signal Processing and Control, 2022.

[21] Fei, Nanyi, Yizhao Gao, Zhiwu Lu, and Tao Xiang. "Z-score normalization, hubness, and few-shot learning." In Proceedings of the IEEE/CVF International Conference on Computer Vision, pp. 142-151. 2021.

[22] Velugoti, S., Reddy, R. H., Tarannum, S., & Reddy, S. T. K. (2022). Lung Nodule Detection and Classification using Image Processing Techniques. International Journal of Computer Engineering In Research Trends, 9(7), 114-119.

[23] Kumar, Vijay, and Priyanka Gupta. "Importance of statistical measures in digital image processing." International Journal of Emerging Technology and Advanced Engineering 2, no. 8 (2012): 56-62.

[24] Shang Lei, "A Feature Selection Method Based on Information Gain and Genetic Algorithm", 2012 International Conference on Computer Science and Electronics Engineering.

[25] Huichao Hong, Shuwan Pan and Lixin Zheng, "A fast calculation method for gray-level co-occurrence matrix base on GPU," 2017 2nd International Conference on Image, Vision and Computing (ICIVC), 2017, pp. 1063-1067, doi: 10.1109/ICIVC.2017.7984717.

[26] A. Hafiane, K. Palaniappan and G. Seetharaman, "Adaptive Median Binary Patterns for Texture Classification," 2014 22nd International Conference on Pattern Recognition, 2014, pp. 1138-1143, doi: 10.1109/ICPR.2014.205.

[27] Alile, S. O., & Bello, M. E. (2020). Diagnosing Chronic Obstructive Pulmonary Disease (COPD) Using Bayesian Belief Network. International Journal of Computer Engineering In Research Trends, 7(6), 1-12..

[28] Sudha D and M Ramakrishna, "Comparative Study of Features Fusion Techniques", 2017 International Conference on Recent Advances in Electronics and Communication Technology.

[29] Meng Cai, Yongzhe Shi and Jia Liu, "Deep Maxout Neural Networks For Speech Recognition", 2013.

[30] Sushma Jaiswal, & Priyanka Gupta. (2023). Ensemble based Model for Diabetes Prediction and COVID-19 Mortality Risk Assessment in Diabetic

Patients. International Journal of Computer Engineering in Research Trends, 10(3), 99–106.

[31] Rudra Kumar, M., Pathak, R., & Gunjan, V. K. (2022). Diagnosis and Medicine Prediction for COVID-19 Using Machine Learning Approach. In Lecture Notes in Electrical Engineering (pp. 123–133). Springer Nature Singapore.

[32] Adhiyaman Manickam, Jianmin Jiang, Yu Zhou, Abhinav Sagar, Rajkumar Soundrapandiyan, R. Dinesh Jackson Samuel,"Automated pneumonia detection on chest X-ray images: A deep learning approach with different optimizers and transfer learning architectures", Measurement, vol.184, 2021

[33] Swetha, A. ., Lakshmi, M. S. ., & Kumar, M. R. . (2022). Chronic Kidney Disease Diagnostic Approaches using Efficient Artificial Intelligence methods. International Journal of Intelligent Systems and Applications in Engineering, 10(1s), 254.

[34] Sravani Nalluri, “Pneumonia Screening on Chest X-Rays with Optimized Ensemble Model”, in communication.

[35] Dinakar, J. R. ., & S., V. . (2023). Real-Time Streaming Analytics using Big Data Paradigm and Predictive Modelling based on Deep Learning . International Journal on Recent and Innovation Trends in Computing and Communication, 11(4s), 161–165. https://doi.org/10.17762/ijritcc.v11i4s.6323

[36] Saini, D. J. B. ., & Qureshi, D. I. . (2021). Feature Extraction and Classification-Based Face Recognition Using Deep Learning Architectures. Research Journal of Computer Systems and Engineering, 2(1), 52:57. Retrieved from https://technicaljournals.org/RJCSE/index.php/journal/article/view/23

[37] Kumbhkar, M., Shukla, P., Singh, Y., Sangia, R. A., & Dhabliya, D. (2023). Dimensional reduction method based on big data techniques for large scale data. Paper presented at the 2023 IEEE International Conference on Integrated Circuits and Communication Systems, ICICACS 2023, doi:10.1109/ICICACS57338.2023.10100261 Retrieved from www.scopus.com